HHS Public Access

Author manuscript

Cell Mol Bioeng. Author manuscript; available in PMC 2017 December 01.

Published in final edited form as:

Cell Mol Bioeng. 2016 December ; 9(4): 538–545. doi:10.1007/s12195-016-0452-9.

Improvement in Electrotransfection of Cells Using Carbon-Based Electrodes

Chun-Chi Chang[1], **Mao Mao**[1], **Yang Liu**[1,2], **Mina Wu**[1], **Tuan Vo-Dinh**[1,2], and **Fan Yuan**[1]

[1]Department of Biomedical Engineering, Duke University, Durham, North Carolina, USA.

[2]Department of Chemistry, Duke University, Durham, North Carolina, USA.

Abstract

Electrotransfection has been widely used as a versatile, non-viral method for gene delivery. However, electrotransfection efficiency (eTE) is still low and unstable, compared to viral methods. To understand potential mechanisms of the unstable eTE, we investigated effects of electrode materials on eTE and viability of mammalian cells. Data from the study showed that commonly used metal electrodes generated a significant amount of particles during application of pulsed electric field, which could cause precipitation of plasmid DNA from solutions, thereby reducing eTE. For aluminum electrodes, the particles were composed of aluminum hydroxide and/or aluminum oxide, and their median sizes were 300 to 400 nm after the buffer being pulsed 4 to 8 times at 400 V cm^{-1}, 5 ms duration and 1 Hz frequency. The precipitation could be prevented by using carbon (graphite) electrodes in electrotransfection experiments. The use of carbon electrodes also increased cell viability. Taken together, the study suggested that electrodes made of inner materials were desirable for electrotransfection of cells *in vitro*.

Keywords

electrotransfection; electro-gene delivery; electroporation; carbon electrodes; DNA precipitation

Introduction

Pulsed electric field has been widely used for introduction of exogenous molecules into cells.[27, 28] Particularly, it can facilitate transfection of cells with plasmid DNA (pDNA). The method, known as electroporation or electrotransfection, was first demonstrated in 1982 by Neumann and colleagues with mouse lyoma cells,[18] and since then has been utilized to introduce a variety of genes into many different cell types both *in vitro*[4, 20] and *in vivo*.[9, 19] Furthermore, electrotransfection has been explored for therapeutic

Corresponding author: Fan Yuan, Ph.D., Department of Biomedical Engineering, 136 Hudson Hall, Box 90281, Duke University, Durham, NC27708, (919) 660-5411 (phone), (919) 684-4488 (fax), fyuan@duke.edu.

Conflicts of Interest

Chun-Chi Chang, Mao Mao, Yang Liu, Mina Wu, Tuan Vo-Dinh, and Fan Yuan declare that they have no conflicts of interest.

Ethical Standards

No human or animal studies were carried out by the authors for this article.

applications,[1, 2, 5-7, 11, 26, 31] including recent Phase I/II clinical trials for cancer treatment and vaccination of infectious diseases.[8]

As a non-viral method, electrotransfection boasts the benefits of low cost, easy and safe to use, and independence of cell surface receptors. It is also capable to deliver a wide spectrum of genes with different sizes. However, the current method has two major limitations. One is low and unstable transfection efficiency; and the other is adverse effects on transfected cells. For example, electrotransfection can lead to cell-cycle arrest and apoptosis,[14] and may cause damage of genomic DNA in cells,[16] presumably due to reactive oxygen species (ROS) generated during pulse application.[25] Another adverse effect is related to metal ions when metal electrodes are used for pulse application. When a large amount of these ions are introduced into cells, they can result in biochemical conversion of inositol phosphates into a form that catalyzes release of excess Ca^{2+}, thereby disturbing intracellular signaling.[15] In addition to the adverse effects on cells, the metal ions interact with various biological macromolecules, including nucleic acids and proteins, causing them to precipitate from solutions.[13, 24] The precipitation will reduce the availability of pDNA for cell transfection. To reduce the undesired effects, we investigated the use of carbon electrodes for electrotransfection. Data from the study showed that carbon electrodes, as an inert and less reactive alternative to metal electrodes, could prevent pDNA from precipitation, and increase cell viability and electrotransfection efficiency (eTE) *in vitro*.

Materials and Methods

Cell culture and plasmid

B16F10, a murine melanoma cell line, was selected for the study. The cells were subcultured every 1-2 days, at 37°C with 5% CO_2 in DMEM (Life Technologies, Gaithersburg, MD) supplemented with 10% FBS (Hyclone, Logan, UT) and penicillin/streptomycin (Life Technologies). The plasmid encoding enhanced green fluorescent protein (EGFP) (pEGFP-N1, Clontech, Palo Alto, CA) was used for all electrotransfection experiments. For visualization, some pDNA molecules were covalently labeled with tetramethyl-rhodamine (LabelIT, Mirus, Madison, WI); and the labeled pDNA was purified through ethanol precipitation and resuspension in water before use.

Carbon and aluminum electrode assemblies

To directly compare electrodes with different materials, we constructed two types of cuvettes that were identical in all parts except for the materials of the plate electrodes (see Figure 1), which were either carbon (GraphiteStore.com, Inc., Buffalo Grove, IL) or aluminum. The aluminum plates were obtained through disassembling a commercial aluminum cuvette (Bio-Rad, Hercules, CA). The two parallel plates were separated by a spacer of 3 mm thick, placed on top of the polydimethylsiloxane (PDMS), and fixed on the cuvette after the entire assembly was baked at 65°C overnight. The spacer was removed before use.

Treatment of solutions with pulsed electric field

To investigate effects of electric pulse treatment on pDNA aggregation, we prepared pDNA (30 or 50 μg ml^{-1}) and tetramethyl-rhodamine labeled pDNA (30 μg ml^{-1}) solutions with

the HeBS buffer (20 mM HEPES, 137 mM NaCl, 5 mM KCl, 0.7 mM Na2HPO4, 6 mM Dextrose) at pH 7.05. Some of these solutions were supplemented with a chelating reagent (citric acid (CA) at 1.875 mg ml^{-1} or EDTA at 1 mM). All solutions were placed on ice before use. In experiments, 100 μl of a solution was removed from the ice, placed in an aluminum cuvette (Bio-Rad, Hercules, CA), and immediately treated with electric pulses using a BTX ECM 830 Square Wave Electroporation System (Harvard Apparatus). The field strength, pulse duration, and pulse interval in all experiments were 400 V cm^{-1}, 5 ms, and 1 sec, respectively; and the number of pulses varied in experiments. After pulsing, the solutions were analyzed by electrophoresis. In addition, the solution with tetramethyl-rhodamine labeled pDNA was centrifuged at 10,000 g for 10 min; and 90 μl supernatant was discarded. The remaining sample was imaged with a 20x objective under a fluorescence microscope.

Electrotransfection

Cultured cells at 70% confluency were collected after trypsinization to prepare single cell suspension with the pDNA solutions prepared above. Cell suspensions (10^6 cells per 100 μl) were transferred into aluminum or carbon cuvettes (see Figure 1) and incubated on ice for 5 min. Then, the samples were pulsed under the same conditions as those described above. After pulsing, the samples were left in the cuvettes at room temperature for 10 min, allowing cell membrane to recover, transferred to 6-well plates, and cultured with 2 ml complete medium at 37°C with 5% CO_2. The eTE and viability of the pulsed cells were further analyzed using flow cytometry.

Characterization of electric pulse induced precipitates

HeBS buffer without pDNA was pulsed 8 times in an aluminum cuvette (Bio-Rad, Hercules, CA) under the conditions described above. The solutions were centrifuged at 10,000 g for 10 min; and the pellets were collected and washed 3 times with DI water to remove soluble salts from the HeBS buffer, and dried in oven at 65°C overnight. Completely dried samples were analyzed by x-ray photoelectron spectroscopy (XPS) in the Shared Materials Instrumentation Facility at Duke University. Chemical compositions were identified by comparing peak binding energies of the samples with the reference peak energies of known compounds.[12] For size and concentration analyses, HeBS buffer with or without pDNA were pulsed 0, 4, or 8 times in aluminum cuvettes (Bio-Rad, Hercules, CA). After the samples were diluted 1:100 with non-pulsed HeBS buffer, concentration distribution of particles with different sizes (between 5 and 1005 nm) in a fixed volume was measured with a nanoparticle tracking system (NS 500, NanoSight, UK). The concentration distribution was integrated to determine the cumulative concentration C_k ($k = 1, 2, ..., K$) by $\sum_{i=1}^{i=k} c_i$, where c_i is the concentration of particles with diameters between d_{i-1} and d_i, $d_0 = 0$, and K is the total number of concentration data in the distribution. The value of d at which C reached 50% of its maximum level was defined as the median particle size in the sample. It was determined by two surrounding pairs of data (d_k vs. C_k) via linear interpolation. The concentration distribution data were also used to determine the size-weighted average concentration C_d by

$\sum_{i=1}^{i=K} d_i c_i / \sum_{i=1}^{i=K} d_i$. Three independent samples were analyzed, and for each sample, the measurements were repeated 5 times and the results were averaged for further analysis.

Flow cytometry for eTE and cell viability

After electrotransfection, cells were incubated for 4 or 24 hours, washed with PBS, and collected after trypsinization. The cell pellet was re-suspended in 300 μl complete medium supplement with 5 μg ml^{-1} propidium iodide (PI) to stain dead cells. The samples were analyzed with a BD FACSCanto II flow cytometer (Becton Dickinson, Franklin Lakes, NJ) at the Duke Cancer Institute Core Research Facility, which was equipped with 488 and 633 nm lasers for simultaneous detection of GFP and PI fluorescence. Forward and side light scatterings were used as independent variables to exclude debris and isolate the cell population of interest. Compensation was set according to the control sample to resolve spectral emission overlap between the two detection channels. For eTE, 10,000 events were collected for each sample. A single cell analysis software (FlowJo, Ashland, OR) was used for data acquisition and analysis. The apparent eTE was defined as the percentage of total viable cells (PI negative) that expressed GFP (PI negative, GFP positive). For cell viability measurement, flow cytometry signals were recorded for 30 sec to make sure that over 10,000 events were collected for each sample. The viability was calculated as the ratio of viable cell (PI negative) numbers between pulsed sample and non-pulsed control because both groups started with the same number of cells. The actual eTE was defined as the percentage of viable cells expressing GFP (PI negative, GFP positive), relative to the total number of viable cells (PI negative) without pulsing. It was calculated as the product of the apparent eTE and the cell viability at 24 hours.

Statistics

Differences in cell viability and eTE between two electrode groups were evaluated with the Wilcoxon Signed Rank test (GraphPad Prism). The data in the two groups were paired because they shared the same cell samples. A difference was considered to be statistically significant if the p-value was less than 0.05.

Results

Electric pulsing-induced precipitates and pDNA aggregation

Application of electric pulses to HeBS buffer in aluminum cuvette caused formation of insoluble precipitates, which caused the buffer to become increasingly cloudy/opaque with increasing the number of applied pulses. The same phenomenon was also observed when different buffers (e.g., PBS) and metal electrodes (e.g., stainless steel, silver, and gold plated materials) were used in the study (data not shown). To focus the study, we only investigated the issue of precipitation in the HeBS buffer contained in aluminum cuvettes. When pDNA was added into the buffer prior to pulsing, it formed complexes with the precipitates that could be demonstrated through gel electrophoresis (Figure 2A). Two bands representing linear and supercoiled forms of pEGFP-N1, respectively, could be detected in the non-pulsed control samples. However, the amount of soluble pDNA in both forms decreased with increasing the pulse number from 3 to 12. The decrease was due to the formation of pDNA

aggregates that were too large to migrate through the agarose gel. To investigate if the precipitation was caused by Al^{3+} ions, we added chelating agents, citric acid (CA) and EDTA, to the HeBS buffer prior to pulsing, and observed that both CA and EDTA could significantly reduce precipitates in the buffer and thus formation of pDNA aggregates (see Figure 2B), indicating that Al^{3+} ions released from electrodes played a key role in the formation of insoluble compounds that caused pDNA aggregation in the buffer. To visualize the aggregates, tetramethyl-rhodamine-labeled pEGFP-N1 was pulsed 0-12 times using aluminum electrodes. Fluorescence images of pDNA obtained shortly after pulsing showed that the size of aggregates increased substantially with increasing the number of pulses (see Figure 2C).

Characterization of electric pulsing-induced precipitates

HeBS buffer was known to contain several elements, such as carbon, oxygen, nitrogen, sodium, and chloride. We confirmed this information with the XPS analysis. After the buffer was pulsed 8 times in aluminum cuvettes, the binding energy profile was analyzed again with the XPS method. We observed that the peak energy of the pulsed samples in the range between 68 and 88 eV occurred at 74.2 eV (Figure 3A), which was slightly higher than that of the metal form of aluminum, Al 2p (72.7 eV), indicating that the precipitate was Al-O and/or Al-OH.[12]

In addition to the chemical composition analysis, we quantified size distributions of the precipitates/particles containing aluminum compounds and pDNA. The cumulative concentration of particles without pDNA was close to zero in the non-pulsed group, but significantly increased after pulsing. The amount of increase was approximately proportional to the number of applied pulses (Figure 3B). When pDNA (50 μg ml^{-1}) was added into the HeBS buffer prior to pulsing, it slightly increased the cumulative concentration in the non-pulsed group, but significantly decreased the difference between the 4- and the 8-pulse groups (Figure 3C). The size-weighted average concentrations of particles are shown in Figure 3D. In addition to the concentrations, we determined median sizes of the particles that were also increased after pulsing (see Figure 3E). It was consistent with the fluorescence images of pDNA aggregates shown in Figure 2C.

Prevention of pDNA precipitation with carbon electrodes

Data shown above indicated that supplementation of the buffer with chelating agents could block formation of precipitates. Although these agents were helpful in elucidating mechanisms of precipitate formation, they can reduce availability of critical ions, such as Ca^{2+}, in cells, causing severe toxicity to pulsed cells. Another approach to blocking pDNA precipitation was to use electrochemically inert electrodes, such as carbon electrodes, for electrotransfection of cells. Using the newly designed carbon cuvette shown in Figure 1, we observed little pDNA aggregates in the samples (see Figure 4), suggesting that carbon electrode would not generate precipitates observed in buffers pulsed with metal electrodes (see Figures 2 and 3).

Improving eTE and cell viability with carbon electrodes

To investigate if the carbon electrode was also less toxic to cells and more efficient for gene delivery, we compared it to aluminum electrode in terms of cell viability and electrotransfection efficiency (eTE). For fair comparisons, we designed and constructed two types of cuvettes with identical dimensions and configurations (see Figure 1). The only difference between the two cuvettes was the electrode materials, which was either carbon or aluminum. Using these cuvettes, we observed little difference in terms of the apparent eTE between the carbon and the aluminum electrodes (see Figure 5A). The cell viabilities in the carbon group, determined at 4 and 24 hours post electrotransfection, were approximately 50% of the values in the non-pulsed controls, but were more than doubled, compared to those in the aluminum group (see Figure 5B). As a result, the actual eTE, calculated as the product of the cell viability and the apparent eTE, was 150% higher in the carbon group than in the aluminum group (see Figure 5C).

Discussion

Results from the study showed that electrotransfection with aluminum electrodes induced formation of precipitates consisting of Al-O and/or Al-OH. The precipitates could bind to pDNA that significantly reduced concentration of free pDNA molecules in the buffer available for transfection. To solve this problem, we designed and constructed a prototype carbon cuvette that could prevent precipitate formation, improve cell viability, and increase eTE.

Significant efforts have been made in previous studies to improve the efficiency of electrotransfection. Most of them are focused on optimization of pulse parameters[7, 17] or pulsing buffers.[10, 23] In this study, we showed that electrode materials could also be modified to enhance the efficiency in *in vitro* studies. Based on this study and those in the literature, metal electrodes, used currently in the majority of commercial products for electrotransfection, can reduce eTE through three potential mechanisms: (i) aggregation of pDNA that reduced the amount of free pDNA molecules available for transfecting cells , (ii) damage of molecular structures in pDNA that might affect transgene expression,[25] and (iii) production of chemicals in the buffer that are toxic to cells.

DNA aggregation

Although the phenomenon of pDNA aggregation has been observed previously,[13, 24] mechanisms of the aggregation are still unknown. In the current study, we demonstrated that the aggregation was caused by Al-O and/or Al-OH released into the buffer during electrotransfection. It is well known that electrolytic reactions at the aluminum anode can release Al^{3+} ions into the buffer. Meanwhile, hydroxyl and oxide ions can be produced at the cathode. Since oxide ions have a relatively short half-life, most Al^{3+} ions would react with hydroxyl ions to produce aluminum hydroxides that were insoluble in water. The precipitates would grow in size to form large amorphous particles (see Figure 3), and bind to nucleotides to cause pDNA aggregation. Although the aggregated pDNA could be still internalized by cells through macropinocytosis,[3, 22] transgenes expression in cells would not

happen if pDNA could not dissociate from the aggregates, escape from endosomes, and enter the nucleus. Therefore, pDNA aggregation alone could reduce eTE.

Cytotoxicity

The current study showed that the viability of cells pulsed with the aluminum electrodes was only half of that pulsed with the carbon electrodes (see Figure 5B). Although we do not know mechanisms of the toxicity, they are likely to be related to aluminum ions and compounds generated during electrotransfection. The ions can easily diffuse into cells via transient pores in plasma membrane created by electric pulses to disturb intracellular environment, which may adversely affect cell viability and transgene expression. The aluminum compounds could form insoluble nano- and micro-particles in the buffer, and be internalized by cells via endocytic pathways. Additionally, the precipitates were positively charged, which could bind to negative charged cell membrane[3, 29]. At high concentrations, these particles could destabilize plasma membrane and induce cell apoptosis.[21, 30]

The problems of pDNA aggregation and aluminum associated cytotoxicity could be circumvented by using carbon electrodes. Our data indicated that the carbon electrodes could successfully prevent pDNA from aggregation (Figure 4) and double the cell viability (Figure 5B), compared with the aluminum electrodes. As a result, the percent of cells that were transfected successfully, or the actual eTE, was improved by a factor of 2.5 (Figure 5C). Taken together, our data demonstrated that electrode materials could be optimized for enhancing eTE.

Acknowledgments

The work was supported partly by grants from National Institutes of Health (GM098520) and National Science Foundation (BES-0828630).

References

1. Ayuni EL, Gazdhar A, Giraud MN, Kadner A, Gugger M, Cecchini M, Caus T, Carrel TP, Schmid RA, Tevaearai HT. In vivo electroporation mediated gene delivery to the beating heart. PloS one. 2010; 5:e14467. [PubMed: 21209934]
2. Bodles-Brakhop AM, Heller R, Draghia-Akli R. Electroporation for the delivery of DNA-based vaccines and immunotherapeutics: current clinical developments. Molecular therapy : the journal of the American Society of Gene Therapy. 2009; 17:585–592. [PubMed: 19223870]
3. Chang C-C, Wu M, Yuan F. Role of specific endocytic pathways in electrotransfection of cells. Molecular Therapy — Methods & Clinical Development. 2014; 1:14058–8. [PubMed: 26052524]
4. Eynard N, Rols MP, Ganeva V, Galutzov B, Sabri N, Teissie J. Electrotransformation pathways of procaryotic and eucaryotic cells: recent developments. Bioelectrochemistry and Bioenergetics. 1997; 44:103–110.
5. Gothelf A, Gehl J. Gene electrotransfer to skin; review of existing literature and clinical perspectives. Current Gene Therapy. 2010; 10:287–299. [PubMed: 20557284]
6. Hargrave B, Downey H, Strange RJ, Murray L, Cinnamond C, Lundberg C, Israel A, Chen Y-J, Marshall WJ, Heller R. Electroporation-mediated gene transfer directly to the swine heart. Gene therapy. 2013; 20:151–157. [PubMed: 22456328]
7. Heller LC, Heller R. In vivo electroporation for gene therapy. Human gene therapy. 2006; 17:890–897. [PubMed: 16972757]

8. Heller R, Heller LC. Gene electrotransfer clinical trials. Advances in genetics. 2015; 89:235–262. [PubMed: 25620013]
9. Heller R, Jaroszeski M, Atkin A, Moradpour D, Gilbert R, Wands J, Nicolau C. In vivo gene electroinjection and expression in rat liver. FEBS Letters. 1996; 389:225–228. [PubMed: 8766704]
10. Henshaw J, Mossop B, Yuan F. Enhancement of electric field-mediated gene delivery through pretreatment of tumors with a hyperosmotic mannitol solution. Cancer Gene Therapy. 2010; 18:26–33. [PubMed: 20847751]
11. Jaichandran S, Yap STB, Khoo ABM, Ho LP, Tien SL, Kon OL. In vivo liver electroporation: optimization and demonstration of therapeutic efficacy. Human gene therapy. 2006; 17:362–375. [PubMed: 16544985]
12. Kammerer R, Barth J, Gerken F, Kunz C, Flodstrom SA, Johansson LI. Surface-Binding-Energy Shifts for Sodium, Magnesium, and Aluminum Metals. Phys Rev B. 1982; 26:3491–3494.
13. Kooijmans SAA, Stremersch S, Braeckmans K, De Smedt SC, Hendrix A, Wood MJA, Schiffelers RM, Raemdonck K, Vader P. Electroporation-induced siRNA precipitation obscures the efficiency of siRNA loading into extracellular vesicles. Journal of controlled release : official journal of the Controlled Release Society. 2013; 172:229–238. [PubMed: 23994516]
14. Lepik D, Jaks V, Kadaja L, Varv S, Maimets T. Electroporation and carrier DNA cause p53 activation, cell cycle arrest, and apoptosis. Analytical biochemistry. 2003; 318:52–59. [PubMed: 12782031]
15. Loomis-Husselbee JW, Cullen PJ, Irvine RF, Dawson AP. Electroporation can cause artefacts due to solubilization of cations from the electrode plates. Aluminum ions enhance conversion of inositol 1,3,4,5-tetrakisphosphate into inositol 1,4,5-trisphosphate in electroporated L1210 cells. The Biochemical journal. 1991; 277(Pt 3):883–885. [PubMed: 1872818]
16. Meaking WS, Edgerton J, Wharton CW, Meldrum RA. Electroporation-induced damage in mammalian cell DNA. Biochimica et biophysica acta. 1995; 1264:357–362. [PubMed: 8547324]
17. Mir LM, Bureau MF, Gehl J, Rangara R, Rouy D, Caillaud JM, Delaere P, Branellec D, Schwartz B, Scherman D. High-efficiency gene transfer into skeletal muscle mediated by electric pulses. Proceedings of the National Academy of Sciences. 1999; 96:4262–4267.
18. Neumann E, Schaefer-Ridder M, Wang Y, Hofschneider PH. Gene transfer into mouse lyoma cells by electroporation in high electric fields. The EMBO Journal. 1982; 1:841–845. [PubMed: 6329708]
19. Nishi T, Yoshizato K, Yamashiro S, Takeshima H, Sato K, Hamada K, Kitamura I, Yoshimura T, Saya H, Kuratsu J, Ushio Y. High-efficiency in vivo gene transfer using intraarterial plasmid DNA injection following in vivo electroporation. Cancer research. 1996; 56:1050–5. [PubMed: 8640760]
20. Potter H, Weir L, Leder P. Enhancer-dependent expression of human kappa immunoglobulin genes introduced into mouse pre-B lymphocytes by electroporation. Proceedings of the National Academy of Sciences. 1984; 81:7161–7165.
21. Rhaese S, von Briesen H, Rubsamen-Waigmann H, Kreuter J, Langer K. Human serum albumin-polyethylenimine nanoparticles for gene delivery. Journal of controlled release : official journal of the Controlled Release Society. 2003; 92:199–208. [PubMed: 14499197]
22. Rosazza C, Phez E, Escoffre JM, Cezanne L, Zumbusch A, Rols MP. Cholesterol implications in plasmid DNA electrotransfer: Evidence for the involvement of endocytotic pathways. International journal of pharmaceutics. 2012; 423:134–43. [PubMed: 21601622]
23. Saulis G, Lapė R, Pranevičiūtė R, Mickevičius D. Changes of the solution pH due to exposure by high-voltage electric pulses. Bioelectrochemistry. 2005; 67:101–108. [PubMed: 15967404]
24. Stapulionis R. Electric pulse-induced precipitation of biological macromolecules in electroporation. Bioelectrochemistry and Bioenergetics. 1999; 48:1–6.
25. Tamiya E, Nakajima Y, Kamioka H, Suzuki M, Karube I. DNA cleavage based on high voltage electric pulse. FEBS Letters. 1988; 234:357–361. [PubMed: 2839372]
26. Touchard E, Berdugo M, Bigey P, El Sanharawi M, Savoldelli M, Naud M-C, Jeanny J-C, Behar-Cohen F. Suprachoroidal electrotransfer: a nonviral gene delivery method to transfect the choroid and the retina without detaching the retina. Molecular therapy : the journal of the American Society of Gene Therapy. 2012; 20:1559–1570. [PubMed: 22252448]

27. Venslauskas MS, Šatkauskas S. Mechanisms of transfer of bioactive molecules through the cell membrane by electroporation. European Biophysics Journal. 2015; 44:1–13. [PubMed: 25391339]
28. Wolff, JA., Budker, V. The Mechanism of Naked DNA Uptake and Expression. Elsevier; 2005. p. 1-20.
29. Wu M, Yuan F. Membrane binding of plasmid DNA and endocytic pathways are involved in electrotransfection of mammalian cells. PloS one. 2011; 6:e20923. [PubMed: 21695134]
30. Xu ZP, Walker TL, Liu K.-l. Cooper HM, Lu GQM, Bartlett PF. Layered double hydroxide nanoparticles as cellular delivery vectors of supercoiled plasmid DNA. International journal of nanomedicine. 2007; 2:163–174. [PubMed: 17722544]
31. Zhou R, Norton JE, Zhang N, Dean DA. Electroporation-mediated transfer of plasmids to the lung results in reduced TLR9 signaling and inflammation. Gene therapy. 2007; 14:775–780. [PubMed: 17344904]

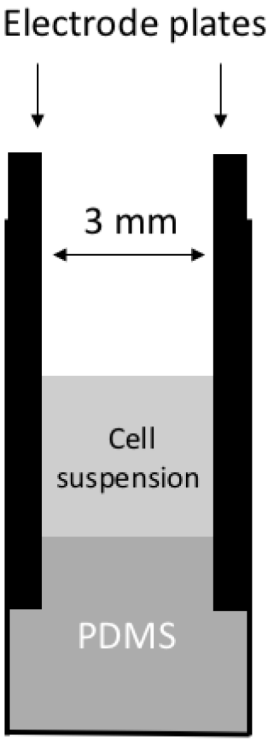

Figure 1.
Schematic of the cuvette design. It consisted of two parallel-plate electrodes. Both plates were made of either graphite carbon or aluminum metal, and fixed in the plastic cuvettes with PDMS.

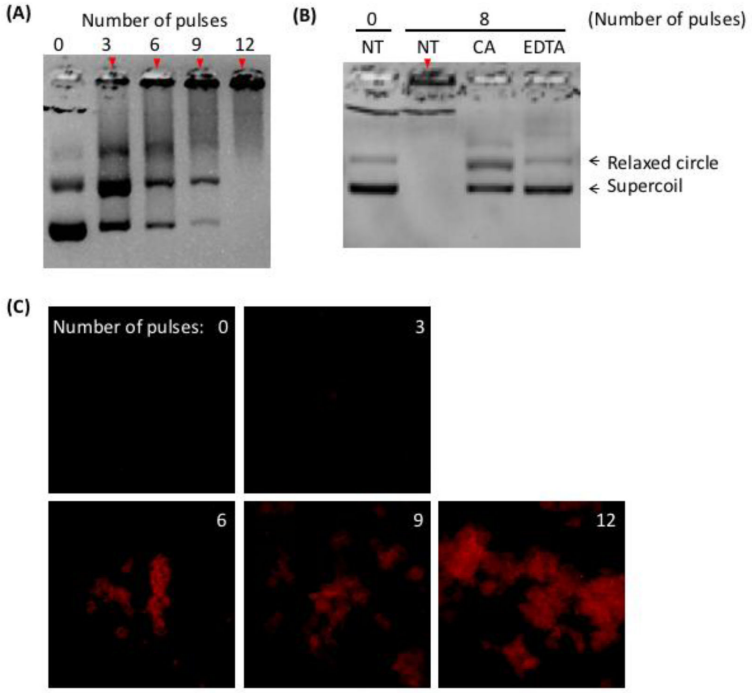

Figure 2.

pDNA aggregation after being pulsed in aluminum cuvettes. (A) Gel electrophoresis of pDNA samples after they were treated with electric pulses at 400 V cm^{-1}, 5 ms duration and 1 Hz frequency in the cuvettes. The number of pulses varied between zero (i.e., the control) and 12. (B) Gel electrophoresis of pDNA samples after they were pulsed in the same buffer supplemented with a chelating agent, citric acid (CA) or EDTA. Solid arrows in both Panels indicate pDNA aggregates in the loading wells. (C) Visualization of pulsed pDNA. Tetramethyl-rhodamine labeled pDNA solution was pulsed in aluminum cuvettes. The number of pulses varied between zero (i.e., the control) and 12 as indicated in the panels. The pulsed samples were imaged under a fluorescence microscope equipped with a 20x objective.

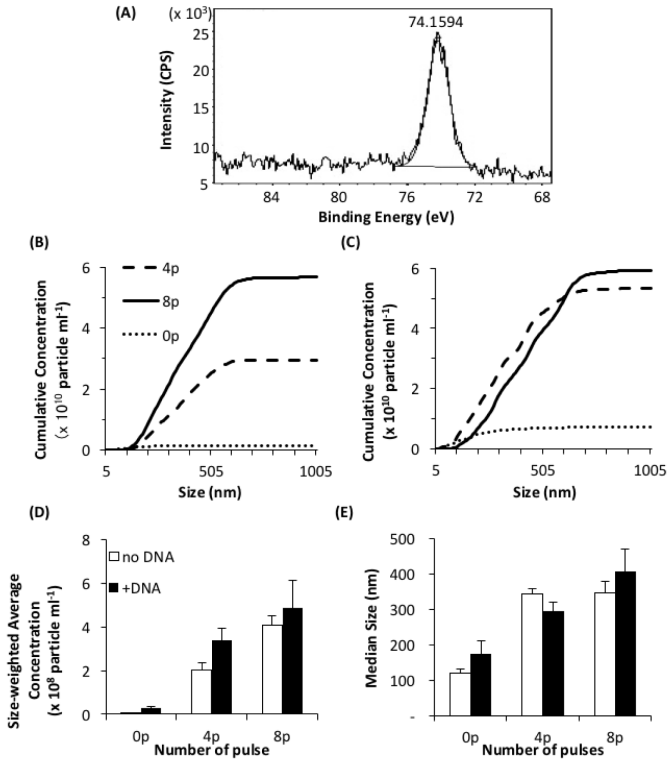

Figure 3.

Characterization of precipitates in the HeBS buffer after being pulsed in aluminum cuvettes. (A) High-resolution XPS spectrum of the precipitates near the peak of binding energy for Al 2p. A dried pellet of precipitates was collected from pulsed buffer, and analyzed with XPS. The peak of the binding energy occurred at 74.2 eV. In Panels (B) through (E), the samples were pulsed 0, 4, or 8 times at 400 V cm^{-1}, 5 ms duration and 1 Hz frequency, diluted 100 times, and analyzed by the nanoparticle tracking system. All data presented these panels are the means from three repeated experiments. Cumulative concentrations of the particles without and with pDNA are shown in (B) and (C), respectively. The size-weighted average concentrations and the median sizes of the particles are shown in (D) and (E), respectively. Open and solid bars represent data without and with pDNA, respectively. The bar and error bar represent the mean and the standard error of the mean (n = 3), respectively.

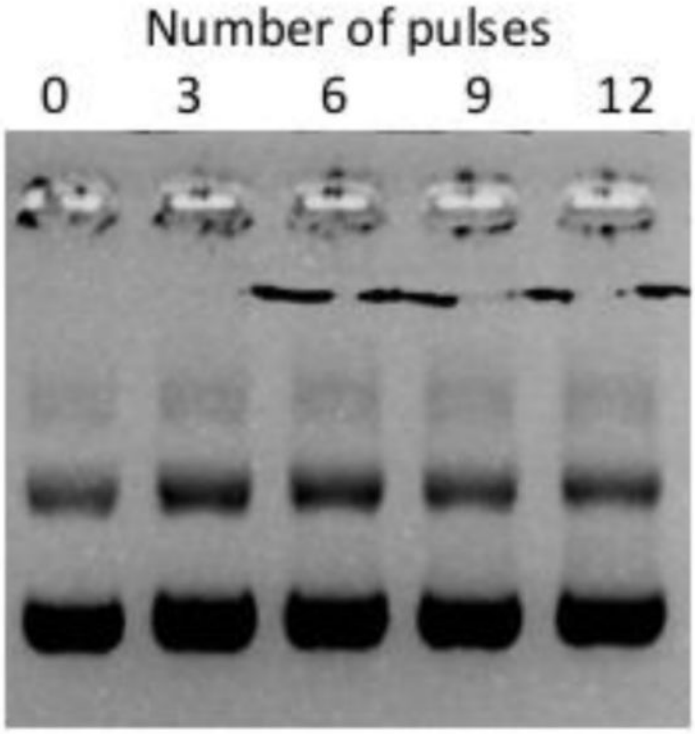

Figure 4.

Prevention of pDNA aggregation using carbon cuvettes. Gel electrophoresis of pDNA after the samples were pulsed 0 to12 times at 400 V cm^{-1}, 5 ms duration, and 1 Hz frequency in carbon cuvettes.

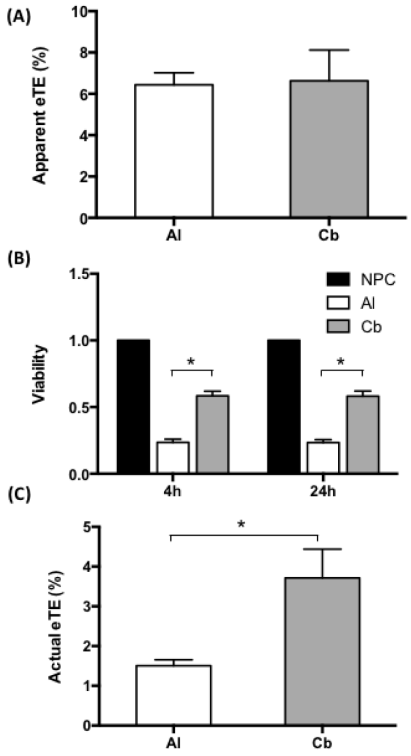

Figure 5.

Effects of electrode materials on cell viability and eTE. (A) Direct comparison of apparent eTE for aluminum (Al) and carbon (Cb) cuvettes. The data were collected at 24 hours after B16F10 cells were treated with 8 pulses at 400 V cm^{-1}, 5 ms duration, and 1 Hz frequency in aluminum or carbon cuvettes. (B) Cell viability after electrotransfection. The data were collected at 4 or 24 hours after the cells were treated with electric pulses in aluminum or carbon cuvettes, and normalized by those in non-pulsed controls (NPC). (C) Actual eTE. It was calculated as the product of the apparent eTE and the cell viability. In each experiment, the average of triplicate measurements was determined; and the experiment was repeated seven times. The bar and error bar represent the mean and the standard error of the mean (n = 7), respectively. * $P < 0.05$.